Pape IJTECH 2019

by Steven Darmawan

Submission date: 17-Sep-2022 03:08PM (UTC+0700)
Submission ID: 1901927522
File name: ch_ME-800_CFD-Investigation-of-Flow-Over-a-Backwardfacing-St.pdf (1.41M)
Word count: 3889
Character count: 20514

International Journal of Technology 10(2): 280-289
ISSN 2086-9614

CFD INVESTIGATION OF FLOW OVER A BACKWARD-FACING STEP USING AN RNG *k-ε* TURBULENCE MODEL

Steven Darmawan[1*], Harto Tanujaya[1]

[1]*Faculty of Engineering, Universitas Tarumanagara,, Jl. Letjen S. Parman No. 1, Jakarta 11440, Indonesia*

(Received: October 2017 / Revised: December 2018 / Accepted: March 2019)

ABSTRACT

Backward-facing step (BFS) is a benchmarked geometry for visualizing recirculation flow and validating turbulence models. Nowadays, numerical analysis with the CFD method has became more popular and has stimulated research involving CFD without avoiding the experimental method. In this paper, flow over a BFS was numerically investigated with an RNG *k-ε* turbulence model to predict recirculating flow. BFS geometry refers to the geometry proposed by Kasagi & Matsunaga; it is three-dimensional, with inlet Re = 5.540. The paper aims to investigate the performance of the RNG *k-ε* turbulence model over a BFS. Two important parameters were analayzed: the performance of the RNG *k-ε* on the recirculation zone and on the reattachment length. Recirculation flow is presented by the x-velocity for Y = 17.4 mm and Y = 34.9 mm. In these Y-section, the RNG *k-ε* is compared to the STD *k-ε* and both models show the recirculation flow occurred from X = 0 mm to about X = 200 mm. The following results were obtained. The RNG *k-ε* predicted a slightly higher x-velocity component than that predicted by the STD *k-ε*. This result shows that the RNG *k-ε* turbulence model is suitable for predicting recirculation flow on the BFS. The reattachment length was measured by non-dimensional X/h to the x-velocity component with the RNG *k-ε* turbulence model. The analyzed data were taken from X/h = 4.5 to X/h = 10, on the x-velocity component from Y = 17.4 mm. The reattachment point was achieved at X/h = 7.22, close to that achieved by Kasagi & Matsunaga of X/h = 6.51.

Keywords: Backward-facing step; CFD; Reattachment point; Recirculation flow; RNG *k-ε* turbulence model

1. INTRODUCTION

Backward-facing step (BFS) is the one of the most powerful geometries for visualizing flow, validating the performance of turbulence model on recirculating flow (Thangam & Speziale, 1991; Thangam, 1991). Generally, there are two main specific flows in a BFS considered as a benchmarking geometry: the recirculating flow after the expansion zone and the reattachment point reaching near to the outlet zone. The recirculated and swirling flow occurs in many engineering applications well-presented by BFS geometry. This type of flow can be useful or harmful, depending on the application; examples include recirculation flow in electronic devices; recirculation flow in aerodynamics fields; flow around buildings in architectural applications; flow in combustion chambers; and the disadvantage of swirling flow at pipe bends (Mouza et al., 2005; Rouizi et al., 2009; Gautier & Aider, 2014; Ramšak, 2015; Saha & Nandi, 2017; Selimefendigil & Öztop 2017). There remain many turbulent flow phenomena over a BFS which

*Corresponding author's email: stevend@ft.untar.ac.id, Tel.+62215663124; +628128291333
Permalink/DOI: https://doi.org/10.14716/ijtech.v10i2.800

are yet to be explored (Kasagi & Matsunaga 1995; Avancha, 2002).

There are several geometrical aspects to BFS, most of which are non-dimensional parameters, such as step height (h), upstream height (H), the expansion ratio and total length (L). Several papers have investigated turbulent flow over a BFS, with specific cases examined experimentally and/or numerically. A review of these geometry parameters was previously made by (Darmawan, 2016). Experimental method of flow over BFS geometry as done by (Kasagi & Matsunaga, 1995; Gautier & Aider, 2013) and many others involving advanced measurement techniques and recording facilities, which are very costly (Gautier & Aider 2014; Kasagi & Matsunaga 1995). Moreover, flexibility in varying the geometry design, lower cost, and faster and better visualization have made the CFD method more popular over the years, two dimensionally and three dimensionally (Thangam, 1991; Avancha & Pletcher, 2002; Nie & Armaly, 2002; Kanna & Das, 2006; Rouizi et al., 2009; Ramšak, 2015). The growth of commercial CFD codes in the market is also increasing the number of CFD applications, with choices of characteristics, acuration. Turbulence model choice plays an important role in producing the acceptable results, needing a physical flow and mathematical knowledge to perform CFD simulation (Ramdlan et al., 2016). An appropriate turbulence model is needed in order to represent the flow with commercial CFD codes. For example, in 2007 Anwar-ul-Haque et al. assessed the performance of turbulence models on backward-facing step applications (Haque et al., 2007).

Many turbulence models are available, with very wide range characteristics, from zero equation to DNS (Direct Numerical Simulation). The two-equation turbulence models (RANS-based) are often used in research regarding acuration and computational resources compared to more complicated models (Thangam, 1991). The STD k-ε turbulence model is the most used model despite its weakness in presenting swirl-dominated flow (Launder & Spalding, 1974; Lakshminarayana, 1996; Marshall & Bakker, 2003). Another turbulence model based on the two-equation model is the RNG k-ε, with improvement in swirling and recirculating flow by renormalizing small scale eddies compared to the STD k-ε (Yakhot & Orszag, 1986; Thangam & Speziale, 1991; Versteeg & Malalasekera, 2007; Budiarso et al., 2013; Darmawan et al., 2013), Therefore, the RNG k-ε may be appropriate for predicting the recirculation flow and reattachment point of the flow on the BFS geometry.

However, the performance of the RNG k-ε turbulence model needs to be compared with the STD k-ε model, as the most used one, with faster computation and lower computational resources. The results then compared with the experimental results obtained by (Kasagi & Matsunaga 1995). The BFS geometry used here also refers to the geometry proposed by Kasagi and Matsunaga, but the effects of the boundary layer are not considered here. Therefore, this paper aims to investigate the performance of RNG k-ε turbulence model over a BFS. The results may might be used as a reference and may be applied in future research involving flow in BFS geometry.

2. METHODS

2.1. Geometry Model

The BFS model consists of a number of important dimension parameters, most of which can be treated as non-dimensional parameters: *step height (h), upstream height (H),* expansion, and total length (L). The expansion ratio is defined as $(H+h)/H$). The geometry model used here refers to a model proposed by (Kasagi & Matsunaga, 1995). That employed an experimental method on the BFS with a 3D-PTV, with water as the working fluid. Table 1 shows the geometry specification.

Table 1 BFS geometry specification

Backward-facing step geometry			
Step height, h (mm)	Upstream height, h (mm)	Expansion ratio	Total Length, L (mm)
41	81	1.5	82.5H
Width (mm)		20h	
Working fluid	:	Water	

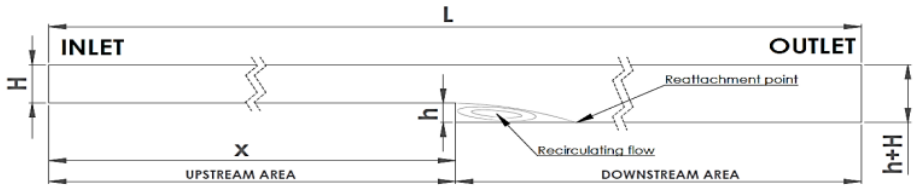

Figure 1 BFS Geometry

2.2. CFD Model

The computational grid that is used for CFD numerical simulation with Autodesk CFD 2017 commercial codes (academic version). Water was used as the working fluid, with the temperature for all four faces of the geometry set at 298K. According to (Kasagi & Matsunaga, 1995), the inlet Reynolds number is set to 5.540, with water as the working fluid. Computation is performed by using a three-dimensional unstructured mesh. Since there are no external forces involved, turbulent intensity is assumed to be 10%. The flow is assumed to be steady-state and the wall is assumed to have zero-roughness. This is also confirmed by the experimental study which is part of the numerical study, which used acrylic as the main material of the BFS geometry (Darmawan, 2017) . Furthermore, the surface roughness of the acrylic is very low (0.07 μm), therefore the wall can be assumed to have zero roughness (Rao et al., 2015).

Mesh dependency analysis was conducted, subject to the mass flow rate of two mesh numbers: 3,055 nodes and 10,426 nodes. Table 2 shows that the nodes amount almost not affect the prediction of the mass flow rate. Considering that the computational time needed was only slightly different, the computational grid with 10,426 nodes was chosen, as shown by Figure 2. Figure 3 shows the closer computational mesh from Figure 2 at the expansion zone. The computational boundaries used in both the mesh dependency analysis and actual analysis are follows: water as working fluid with Reynolds number (Re): 5.540 and temperature of 298 K; zero roughness wall; and pressure at the outlet set to 0.1 MPa.

Table 2. Mesh dependency analysis

	RNG k-ε turbulence model			
	Nodes: 3,055		Nodes: 10,426	
	Inlet	Outlet	Inlet	Outlet
Mass flow rate (kg/s)	2.293	-2.288	2.222	-2.288

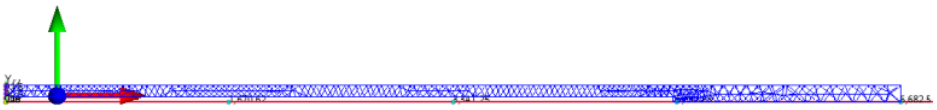

Figure 2 Computational grid of the BFS

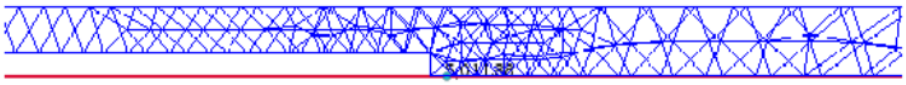

Figure 3 Computational grid at the expansion zone

Governing Equation

As the most common model, the STD *k-ε* turbulence model developed by Launder & Spalding is a two-equation (RANS-based) turbulence model, consisting of *k* and *ε* transport equations for handling turbulence kinetic energy and dissipation respectively (Launder & Spalding 1974)

k transport equation

$$\frac{Dk}{Dt} = \frac{1}{\rho}\frac{\partial}{\partial x_k}\left[\frac{\mu_T}{\sigma_\kappa}\frac{\partial \kappa}{\partial x_k}\right] + \frac{\mu_T}{\rho}\left(\frac{\partial U_i}{\partial x_k} + \frac{\partial U_k}{\partial x_i}\right)\frac{\partial U_i}{\partial x_k} - \varepsilon \quad (1)$$

ε transport equation

$$\frac{D\varepsilon}{Dt} = \frac{1}{\rho}\frac{\partial}{\partial x_k}\left[\frac{\mu_T}{\sigma_\varepsilon}\frac{\partial \varepsilon}{\partial x_k}\right] + \frac{C_1\mu_T}{\rho}\frac{\varepsilon}{k}\left(\frac{\partial U_i}{\partial x_k} + \frac{\partial U_k}{\partial x_i}\right)\frac{\partial U_i}{\partial x_k} - C_2\frac{\varepsilon^2}{\kappa} \quad (2)$$

Model constants

C_μ	C_1	C_2	σ_κ	σ_ε
0.09	1.44	1.92	1.0	1.3

The RNG *k-ε* turbulence model was developed from the STD *k-ε* turbulence model, in which the small-scale eddies are normalized (Renormalization Group) was developed by (Yakhot & Orszag, 1986). Mean flow property and turbulent effects are averaged (Versteeg & Malalasekera, 2007), (TM-107, 1993), (Munson et al., 2009). Reynolds stress governs the eddy viscosity concept, with reference to the Boussinesq equation (Blazek, 2005). With the application of renormalization theory, small scale eddies are computed and averaged separately and then solved together with the large-scale eddies. With this concept, the computational resources needed by the RNG turbulence model are similar to the STD *k-ε*. Recirculation and swirling flows are turbulent flows involving wide range interaction between small- and large-scale eddies. This is the reason why the RNG *k-ε* turbulence model can produce better results than the STD *k-ε* turbulence model in handling recirculation flow. Like the other two-equation turbulence models, the RNG *k-ε* turbulence model consists of *k* and *ε* transport equations for handling turbulence kinetic energy and dissipation respectively.

k transport equation

$$\frac{\partial K}{\partial t} + (\bar{v}.\nabla)K = \frac{\nu_T}{2}\left(\frac{\partial \bar{v}_i}{\partial x_j} + \frac{\partial \bar{v}_j}{\partial x_i}\right)^2 - \bar{\varepsilon} + \frac{\partial}{\partial x_i}\alpha_K \nu_T \frac{\partial K}{\partial x_i} \quad (3)$$

$$\frac{\partial K}{\partial t} + (\bar{v}.\nabla)K = 0.3\left(2\overline{S_{ij}^2}\right)^{1/2} - \bar{\varepsilon} + \frac{\partial}{\partial x_i}\alpha_K \nu_T \frac{\partial K}{\partial x_i} \quad (4)$$

$$\frac{\partial K}{\partial t} + (\bar{v}.\nabla)K = P - \bar{\varepsilon} + \frac{\partial}{\partial x_i}\alpha_K \nu_T \frac{\partial K}{\partial x_i} \quad (5)$$

ε transport equation

$$\frac{D\bar{\varepsilon}}{Dt} = \bar{P} - 1.7215\frac{\bar{\varepsilon}^2}{K} + \frac{\partial}{\partial x_i}\alpha_\varepsilon \nu \frac{\partial \bar{\varepsilon}}{\partial x_i} \quad (6)$$

$$\frac{D\bar{\varepsilon}}{Dt} = -1.063\frac{\bar{\varepsilon}}{K}\tau_{ij}\frac{\partial \bar{v}_i}{\partial x_i} - 1.7215\frac{\bar{\varepsilon}^2}{K} + \frac{\partial}{\partial x_i}\alpha_\varepsilon \nu \frac{\partial \bar{\varepsilon}}{\partial x_i} \quad (7)$$

General form for ε transport eq.

$$\frac{D\bar{\varepsilon}}{Dt} = -C_{\varepsilon 1}\frac{\bar{\varepsilon}}{K}\tau_{ij}\frac{\partial \bar{v}_i}{\partial x_i} - C_{\varepsilon 2}\frac{\bar{\varepsilon}^2}{K} + \frac{\partial}{\partial x_i}\alpha_\varepsilon \nu \frac{\partial \bar{\varepsilon}}{\partial x_i} \quad (8)$$

Model Constants:

C_μ	$C_{\varepsilon 1}$	$C_{\varepsilon 2}$	Pr_t	C_κ	κ	Ba	S_3
0.0845	1.063	1.7215	0.7179	1.617	0.372	1.161	0.478

where C_μ is the total viscosity constant, $C_{\varepsilon 1}$ is the turbulent production constant on dissipation transport, $C_{\varepsilon 2}$ is the dissipation constant on dissipation transport, κ is the von Kármán constant, C_κ is the constant, Ba is the Batchelor constant, S_3 is the matrix skewness factor.

3. RESULTS

CFD simulation was conducted with Autodesk CFD 2017 commercial codes. Figure 4 to Figure 7 show the CFD simulation results with STD k-ε and RNG k-ε The two specific flow parameters on the BFS analysed were recirculation flow and reattachment length, represented by Figure 5 and Figure 7. Based on these reasons, analysis subjected to the v_x velocity component (inlet to outlet direction). The recirculation flow is characterized by the intensity of the reverse direction of the v_x velocity component, while the reattachment length is measured by the distance from the expansion zone start to the point at which the v_x velocity component is reversing (X) compared to step height (h) = (X/h).

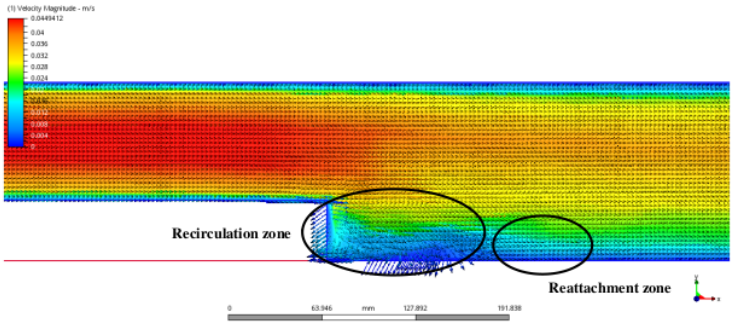

Figure 4 STD k-ε, v_x velocity component

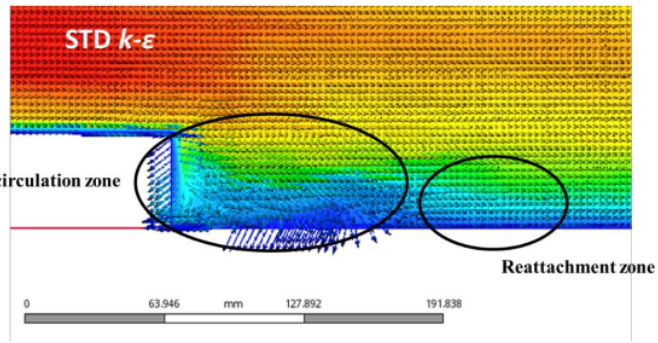

Figure 5 Recirculation and reattachment zone computed with the STD k-ε turbulence model

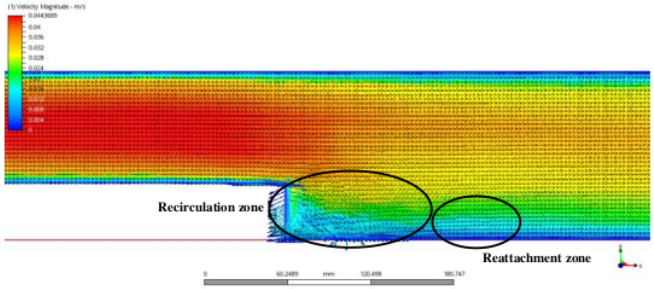

Figure 6 RNG k-ε, v_x velocity component

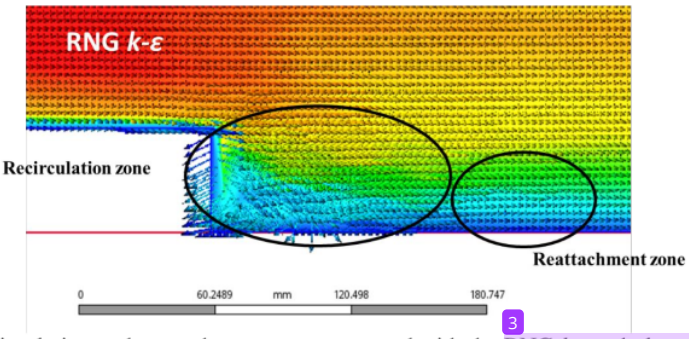

Figure 7 Recirculation and reattachment zone computed with the RNG k-ε turbulence model

3.1. STD k-ε and RNG k-ε Turbulence Model Comparison

Figure 4 and Figure 6 show the x-y plane with the v_x velocity component generated by the STD k-ε and RNG k-ε turbulence models respectively. The plane is located at the midpoint of the BFS width. Since the width of the BFS is large enough and the upstream length is long enough, this plane can be considered to represent the general flow as the flow is fully developed so can be assumed to be a two-dimensional flow. With Re = 5,540, both models show similar results on the v_x velocity component on the upstream zone (inlet zone to the expansion zone). The different shown by the recirculation zone and reattachment length The recirculation zone predicted by the RNG k-ε turbulence model tends to generate more fluctuation between small scale and large scale eddies, with a higher velocity than that generated by the STD k-ε turbulence model. The reattachment zone which reached lower on the RNG k-ε might be caused by the fluctuation predicted by RNG k-ε turbulence model. This phenomenon is in line with the principle of the turbulent flow which resulting an efficient mixing between smaller and larger eddies, cascade energy is decreasing on STD k-ε turbulence model (Tennekes & Lumley, 1972). More detailed results are given in the following section, with the graphical forms.

4. DISCUSSION

4.1. Recirculation Zone

Recirculation flow occurs in the expansion zone, where the fluid flows from the upstream to the downstream zone. Figure 5 and Figure 7 show more detailed analysis made in this area by comparing the results generated by the STD k-ε and RNG k-ε turbulence models on a graph presented by v_x velocity component in the near-wall zone. A higher fluctuation velocity profile is assumed to give a better prediction of the recirculation zone. Figure 8 gives a clearer

understanding of the datum position used in the graphical analysis, with the datum point set on the left-hand corner side of the expanded area.

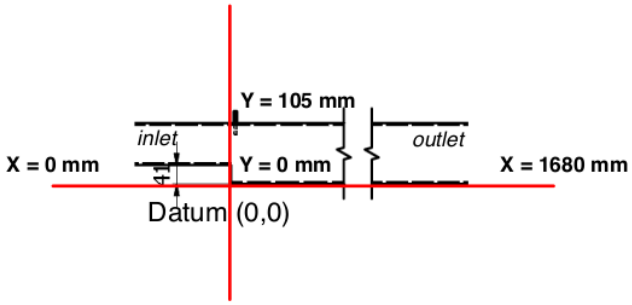

Figure 8 Simplified BFS geometry with datum point

The x-velocity component along the i-direction is presented graphically, starting from the datum point to the outlet side. Two Y-points are considered. Figure 9 and Figure 10 show the velocity profiles at Y = 17.4 mm and Y = 34.9 mm respectively. Both models show that the recirculation flow occurred from X = 0 mm to about X = 200 mm, as shown in Figure 4 and Figure 6. The main reason the STD k-ε turbulence model is used is because of its popularity as a fluid computational method. The velocity profile trend is similar for both models, but a higher x-velocity component is predicted by the RNG k-ε turbulence model than by the STD k-ε turbulence model, meaning that interaction between small- and large-scale eddies is higher, so the velocity is greater. Cascade energy is dominant in this condition, since the recirculation flow is closely related to the interaction between the scales of eddy. The additional terms of the RNG k-ε for both k and ε transport equations undoubtedly make the computational time with this model longer than that of the STD k-ε. Considering the cascade energy concept which larger velocity production represented by turbulent production term in Equation 3, the RNG k-ε turbulence model is more suitable for this type of flow.

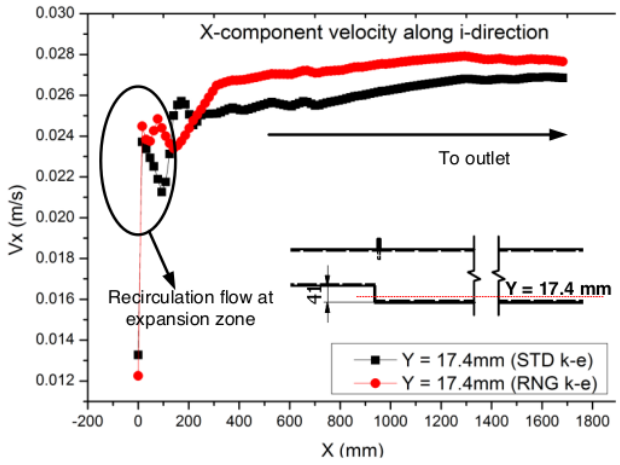

Figure 9 X-component velocity along i-direction, Y = 17.4 mm

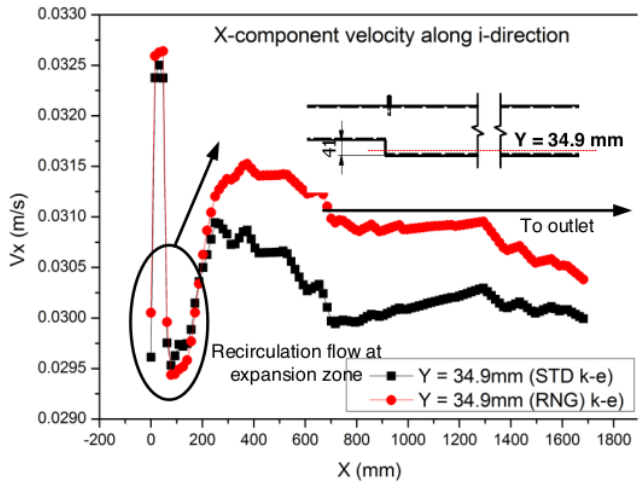

Figure 10 X-component velocity along i-direction, Y = 34.9 mm

4.2. Reattachment Length

It is well-known that reattachment length is one of the most important flow parameters in BFS geometry. Hence, the reattachment point can be defined as the location at which the x-velocity component increases after recirculating and decreases to the outlet side smoothly. According to this definition, the reattachment length is measured by non-dimensional X/h to the x-velocity component. Analyzed data were taken from $X/h = 4.5$ to $X/h = 10$, on the x-velocity component from Y = 17.4 mm, as can be seen in Figure 11. With the RNG k-ε turbulence model, the reattachment point is achieved at $X/h = 7.22$. This approach is different to the definition of Kasagi & Matsunaga, who define reattachment length as the location where the time fraction of forward flow is equal to 0.5 towards the wall (Kasagi & Matsunaga, 1995). However, the result is not far from the $X/h = 6.51$ achieved by Kasagi & Matsunaga. The velocity profile tends to decline steadily after $X/h = 10$.

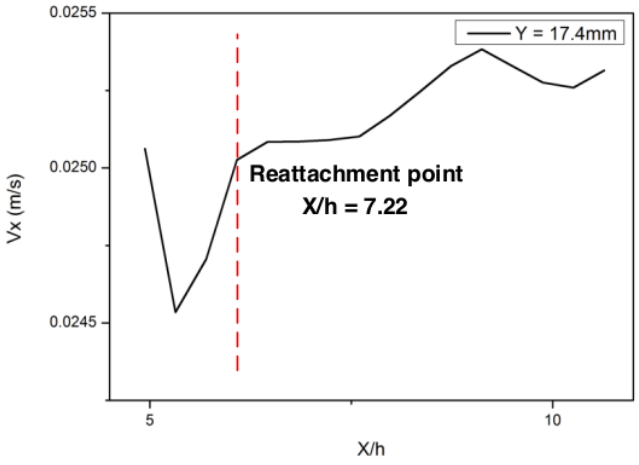

Figure 11 Reattachment length

5. CONCLUSION

A numerical study of the flow over a backward-facing step was conducted with Re = 5.540 with STD *kε* and RNG *k-ε* turbulence models. The conclusions are as follows: (1) The recirculation flow predicted by the RNG *k-ε* turbulence model is higher than that predicted by STD *k-ε* turbulence model in qualitative terms. This was measured by the x-velocity component along the x-direction, which shows that the RNG *k-ε* is better for use in such a flow; and (2) With the RNG *k-ε* turbulence model, at Y = 17.4 mm the reattachment point was achieved at *X/h* = 7.22.

6. ACKNOWLEDGEMENT

The authors would like to thank LPPI (*Lembaga Penelitian dan Publikasi Ilmiah* – Centre of Research and Publication) Universitas Tarumanagara for funding this research through the Hibah Riset Internal – Periode 2, 2016 scheme.

7. REFERENCES

Avancha, R.V.R., Pletcher, R.H., 2002. Large Eddy Simulation of the Turbulent Flow Past a Backward-facing Step with Heat Transfer and Property Variations. *International Journal of Heat and Fluid Flow*, Volume 23(5), pp. 601–614

Blazek, J., 2005. *Computational Fluid Dynamics: Principles and Applications*. 2nd ed. Amsterdam: Elsevier

Budiarso, Siswantara, A.I., Darmawan, S., 2013. *Secondary Flow pada Pipa Keluar Kompresor Turbin Gas Mikro Bioenergi Proto X-2 : Analisis dengan Model Turbulen STD k-ε dan RNG k-ε* (Secondary Flow on Compressor Discharge Pipe of Proto X-2 Bioenergy Micro Gas Turbine: Analysis with STD k- ε and RNG k- ε Turbulence Model) *In:* Seminar Nasional Tahunan Teknik Mesin. Volume XII, pp. 23–24

Darmawan, S., 2017. Experimental Study of Smoke over a Backward-facing Step Geometry. *In:* The 3rd International Conference on Engineering of Tarumanagara, Jakarta: Faculty of Engineering, Universitas Tarumanagara

Darmawan, S., 2016. Backward Facing-step Geometry for Flow Analysis: A Review of Non-dimensional Parameters. *Journal of Academic Faculty Development*, Volume 1(1), pp. 1–11

Darmawan, S., Budiarso, Siswantara, A.I., 2013. CFD Investigation of Standard *k-ε* and RNG *k-ε* Turbulence Model in Compressor Discharge of Proto X-2 Bioenergy Micro Gas Turbine. *In*: The 8th International Conference in Fluid Thermal and Energy Conversion. Semarang

Darmawan, S., Siswantara, A.I., Budiarso, 2013. Comparison of Turbulence Models on Reynolds Number of a Proto X-2 Bioenergy Micro Gas Turbine's Compressor Discharge. *In*: International Conference on Engineering of Tarumanagara, pp. 978–979. Faculty of Engineering, Universitas Tarumanagara

Gautier, N., Aider, J.L., 2013. Control of the Separated Flow Downstream of a Backward-facing Step using Visual Feedback. *Proceedings of the Royal Society A: Mathematical, Physical and Engineering Sciences*, Volume 469(2160), pp. 1–13

Gautier, N., Aider, J.L., 2014. Upstream Open Loop Control of the Recirculation Area Downstream of a Backward-facing Step. *Comptes Rendus - Mecanique*, Volume 342(6–7), pp. 382–388

Haque, A.U., Ahmad. F., Yamada, S., Chaudhry. S.R., 2007. Assessment of Turbulence Models for Turbulent Flow over Backward Facing Step. *The World Congress on Engineering 2007,* Volume II, pp. 1–6

Kanna, P.R., Das, M.K., 2006. Conjugate Heat Transfer Study of Backward-facing Step Flow - A Benchmark Problem. *International Journal of Heat and Mass Transfer,* Volume 49(21-22), pp. 3929–3941

Kasagi, N., Matsunaga, A., 1995. 3-D Particle-tracking Velocimetry Measurement of Turbulence

Statistics and Energy Budget in a Backward-facing Step Flow. *International Journal of Heat and Fluid Flow,* Volume 16(6), pp. 477–478

Lakshminarayana, B., 1996. *Fluid Dynamics and Heat Transfer of Turbomachinery*. New Jersey: John Wiley & Sons, Inc.

Launder, B., Spalding, D.B., 1974. The Numerical Computation of Turbulent Flows. *Computer Methods in Applied Mechanics and Engineering*, Volume 3(2), pp. 269–289

Marshall, E.M., Bakker, A., 2003. *Computational Fluid Mixing*. Lebanon, NH: Fluent, Inc.

Mouza, A.A., Pantzali, M.N., Paras, S.V., Tihon, J., 2005. Experimental and Numerical Study of Backward-facing Step Flow *In:* The 5th National Chemical Engineering Conference, Thessaloniki, Greece

Munson, B.R., Okiishi, T.H., Huebsch, W.W., 2009. *Fundamentals of Fluid Mechanics*. 6th Edition: John Wiley & Sons, Inc.

Nie, J.H., Armaly, B.F., 2002. Three-dimensional Convective Flow Adjacent to Backward-facing Step - Effects of Step Height. *International Journal of Heat and Mass Transfer*, Volume 45(12), pp. 2431–2438

Ramdlan., G.G., Siswantara, A.I., Budiarso, Daryus, A., Pujowidodo, H., 2016. Turbulence Model and Validation of Air Flow in Wind Tunnel. *International Journal of Technology*, Volume 7(8), pp. 1362–1372

Ramšak, M., 2015. Conjugate Heat Transfer of Backward-facing Step Flow: A Benchmark Problem Revisited. *International Journal of Heat and Mass Transfer*, Volume 84, pp. 791–799

Rao, D.C., Kalavathy, N., Mohammad, H.S., Hariprasad, A., Kumar, C.R., 2015. Evaluation of the Surface Roughness of Three Heat ‐ Cured Acrylic Denture Base Resins with Different Conventional Lathe Polishing Techniques : A Comparative Study. *The Journal of Indian Prosthodontic Society,* Volume 15(4), pp. 374–380

Rouizi, Y., Favennec, Y., Ventura, J., Petit, D., 2009. Numerical Model Reduction of 2D Steady Incompressible Laminar Flows: Application on the Flow over a Backward-facing Step. *Journal of Computational Physics,* Volume 228(6), pp. 2239–2255

Saha, S., Nandi, N., 2017. Kinetic Model Development for Biogas Production from Lignocellulosic Biomass. *International Journal of Technology*, Volume 8(4), pp. 681–689

Selimefendigil, F., Öztop, H.F., 2017. Forced Convection and Thermal Predictions of Pulsating Nanofluid Flow over a Backward Facing Step with a Corrugated Bottom Wall. *International Journal of Heat and Mass Transfer,* Volume 110, pp. 231–247

Tennekes, H., Lumley, J.L., 1972. *A First Course in Turbulence*. Massachusetts: MIT Press, Cambridge, Massachusetts, and London, England

Thangam, S., 1991. *Analysis of Two-equation Turbulence Models for Recirculating Flows*. Report 91-61, Institute for Computer Applications in Science and Engineering, NASA, Langley Research Center, Hampton, Virginia

Thangam, S., Speziale, C.G., 1991. Turbulent Separated Flow Past a Backward-facing Step: A Critical Evaluation of Two-equation Turbulence Models. *American Institute of Aeronautics and Astronautics Journal,* Volume 30(10), pp. 2576–2576

TM-107. 1993. *Introduction to the Renormalization Group Method and Turbulence Modeling*. Lebanon, NH: Fluent, Inc.

Versteeg, H.K., Malalasekera, W., 2007. *Introduction to Computational Fluid: The Finite Volume Method*. 2nd edition Essex: Pearson Education Limited, London, England

Yakhot, V., Orszag, S.A., 1986. Renormalization Group Analysis of Turbulence. I. Basic Theory. *Journal of Scientific Computing*, Volume 1(1), pp. 3–51

Pape IJTECH 2019

ORIGINALITY REPORT

9%	5%	10%	3%
SIMILARITY INDEX	INTERNET SOURCES	PUBLICATIONS	STUDENT PAPERS

PRIMARY SOURCES

1	David K. Gartling. "A test problem for outflow boundary conditions—flow over a backward-facing step", International Journal for Numerical Methods in Fluids, 1990 Publication	2%
2	T.L. Chan, G. Dong, C.W. Leung, C.S. Cheung, W.T. Hung. "Validation of a two-dimensional pollutant dispersion model in an isolated street canyon", Atmospheric Environment, 2002 Publication	2%
3	eprints.nottingham.ac.uk Internet Source	1%
4	Peng Xu. "Innovative Hydrocyclone Inlet Designs to Reduce Erosion-Induced Wear in Mineral Dewatering Processes", Drying Technology, 02/2009 Publication	1%
5	Erhan Pulat, Mustafa Kemal Isman, Akın Burak Etemoglu, Muhiddin Can. "Effect of Turbulence Models and Near-Wall Modeling	1%

Approaches on Numerical Results in Impingement Heat Transfer", Numerical Heat Transfer, Part B: Fundamentals, 2011
Publication

6	Submitted to University of Glamorgan Student Paper	1 %
7	Dunn, Matthew C., Babak Shotorban, and Abdelkader Frendi. "Uncertainty Quantification of Turbulence Model Coefficients via Latin Hypercube Sampling Method", ASME 2010 3rd Joint US-European Fluids Engineering Summer Meeting Volume 1 Symposia – Parts A B and C, 2010. Publication	1 %
8	Kasagi, N.. "Three-dimensional particle-tracking velocimetry measurement of turbulence statistics and energy budget in a backward-facing step flow", International Journal of Heat and Fluid Flow, 199512 Publication	1 %

Exclude quotes	On	Exclude matches	< 1%
Exclude bibliography	On		